Chapter 3

Superconducting RF Technology

3.1 Cryomodule, cryogenic thermal balance and quadrupole R&D

Author: **Pierini**, Peterson, Kashikhin

The overall ILC cryogenic scheme evolved from the TESLA superconducting linear collider proposal [1]. The TESLA cryomodule design has been conceived in the late 90s to meet the project requirements of high-filling factors, moderate capital and operation costs and effective alignment and assembly procedures [2]. This module design has been employed for the realization of the TESLA Test Facility (TTF) linac, now operating as the FLASH free electron laser facility in DESY, and was improved in several iterations during the deployment of the facility [3]. The successful TTF design, with minimal modifications, has been later adopted for the linac of the European XFEL, which is composed of 100 modules of this type, and evolved with few variations, into the baseline for the ILC [4, 5].

The energy reach and beam requirements of the ILC require

- a *high filling factor* (the ratio between the real estate gradient and the nominal cavity gradient performances) to reduce the machine footprint.

- *moderate capital and operation cost* per unit length. The first goal is achieved by choosing as much as possible a simple functional design, based on proven and reliable technologies, readily available in the industrial contexts, while the second is obtained by a careful thermal design aimed at minimization of all spurious static losses to the 2 K environment.

- effective beamline components *assembly and alignment procedures*. Cost effective module assembly procedures which are compatible with the cleanliness requirement needed by high gradient bulk-Nb cavity technology are needed. Preservation, reproducibility and stability of the beamline components is a crucial issue for the achievement of beam parameters.

The high filling factor concept favors therefore the choice of long cryomodules (containing several cavities) and their connection in long cryo-units, separated by short interconnections. This aspect, combined with the low loss requests have lead to the integration of the cryogenic cooling circuits into the cryostat cross section. Thus in this scheme the cryomodule, besides providing the usual functions of mechanical support structure for the beamline elements and of isolation from the warm temperature environment, becomes a substantial part of the cryogenic system, since it representes the region where nearly all losses occur and also takes care of the fluid distribution in the linac. In order to perform an overall system optimization, module and cryosystem aspects should be balanced.

The TTF module design has been developed in order to meet the requirements mentioned above and has been extensively characterized, thoroughly tested and operated for years in a linac driving a high availability user facility, at TTF/FLASH. From this design all the DESY FLASH and XFEL linac modules, the FNAL type IV modules for NML and the S1-Global modules at KEK have been derived, with small variations, and manufactured by several industrial producers worldwide.

The ILC module concept therefore builds on a *reliable and mature technology*, currently available in different laboratories worldwide as a result of the ILC S1 and S2 efforts. The already large experience gained at FLASH and at the facilities based on this design will be soon consolidated by the relatively large amount of information coming from the European XFEL Project, which will deploy a 100-module linac at the tunnel installation rate of 1 module per week. The experience that will be accumulated with the 100 XFEL modules production, assembly and operation will be particularly relevant for the further evolutions and the finalization of the ILC concept.

The following subsections briefly resume the recent status of R&D activities worldwide on the further developments, characterization and testing of ILC-class cryomodules carried since the ILC RDR, that helped the identification of a baseline solution for this TDR.

3.1.1 Measurements of the thermal performances of the S1-Global modules

Within the S1-Global [6, 7, 8, 9] international collaboration (reported in section ??), a strong effort was dedicated to the experimental assessment of the thermal performances of the different cryomodule and subcomponent variants [10]. This activity has been motivated by several reasons:

- the exploration of design variants for a possible cost reduction of the mass-produced cryomodules,
- the opportunity given by the experimental activities at KEK to provide a comparison for the thermal performances of the different variations of components integrated in the S1-Global setup,
- the need to benchmark with experimental measurements the design heat load calculations based on engineering calculations and FEM models.

5-K shield simplification studies

One of the original STF modules was used to explore the feasibility and the consequences of removing the inner 5-K shield of the cryomodules, as a possible cost reduction measure, leading to a decrease in fabrication costs and envisaged simplifications of the assembly operations. This concept has been tested at KEK by heat load measurement with and without the shield. Heat loads were measured by means of the evaporated mass flow for the 2-K region and of the shield temperature increase after stopping the coolant for the shield circuits [10].

In the ILC cryomodule both thermal shields provide a manifold for the thermalization of direct conduction paths to the many penetrations reaching the 2-K environment (couplers, HOM, current leads, supports, cables, . . .). Thus a thermal sinking of these conduction paths need to be provided by a circuit at approximately 5-K in order to limit direct heat flow by conduction at 2-K, and therefore a complete elimination of the 5-K shield is not feasible. In the KEK experiments the top shield parts were retained and the bottom shield portions were removed. Heat loads were measured in these two setups (with and without bottom shield portions) to support and validate heat load estimations obtained by means of FEM models, which usually implement simplified heat transfer mechanisms (especially concerning radiation exchange) and suffer by a lack of a reliable dataset for material properties at low temperatures.

The removal of the bottom shields led to an increase of static loads to the 2-K region of approximately 0.8 W in the 6 m S1-Global module, as a consequence of the thermal radiation from the 70 K shield now impinging on the 2 K surfaces. The experimental activity allowed to tune FEM model parameters (e.g. surface emissivities to account for multilayer insulation) in order to explore mitigating actions by means of alternate cooling schemes. Further FEM studies originating from the analysis of these measurements show that the radiation load increase can be avoided by implementing an alternate cryogenic coolant flow scheme with respect to the one foreseen in the RDR. The decrease of the average shield temperature obtained by reverting the coolant flow direction allows to reduce the thermal static load to the coldest temperature level. Thus, by making use of this concept, it is possible to keep the overall static consumption of an ILC module withouth the lower 5-K shield parts to the same level of the nominal RDR design, with a complete 5-K shield.

We have to note, however, that the proper implementation of the cryogenic flow reversal would imply a complete redesign of the module transverse cross section, with redistribution of the cryogenic piping, in order to properly reroute the thermal sinking of the conduction paths. A complete module redesign, even keeping constant nominal heat load performances, could introduce deviations from the consolidated experience achieved by the evolution of these modules and which will be available in the short future for the European XFEL modules. On the basis of these consideration it has been therefore decided to keep in the TDR the nominal cooling scheme as foreseen by the RDR (matching the XFEL modules layout) and leave the possibility for reconsidering the 5K removal/flow inversion possibility at a later engineering stage of the project, together with the finalization and final optimization of the temperature stages of the cryosystems.

Analytic heat load measurements

A second important goal achieved by the S1-Global experimental program has been the study of the static and dynamic thermal performances of the design variants for the components. Such a characterization is important in order to include heat load estimations for the "plug-compatible" components of the ILC cryomodules, to achieve the overall heat load budget available for the cryomodule unit. The two modules of the S1-Global were derived from the joint collaborative work of Fermilab, KEK and INFN for the ILC cryomodules, started in May 2008, which eventually lead to the Type 4 cryomodule design which constitute the ILC baseline. For the S1-Global effort KEK performed the modifications of this design into a half cryomodule (Cryomodule-A), from one of the original STF modules [11] in 2009, while INFN and KEK cooperatively provided components for another half cryomodule, so-called Cryomodule-C. Cryomodule A and C were equipped with a number of different variant of components, i.e. cavity and tuner packages, magnetic shielding, couplers, designed by the different groups participanting in the collaborative work.

The cryomodules and STF cryogenic infrastructure have been instrumented with a large number of sensors to monitor component temperatures and cryogenic flow conditions, in order to assess heat loads at the different circuit levels and compare them with the evaluations, and experimental procedures have been devised to assess individual contributions from the components. Table 3.1 summarizes the good comparison between the static estimations and measurements at S1-Global. As for the case of the 5-K shield studies previously reported, the overall heat loads on the 2-K environment have been derived from the mass flows of the evaporated LHe by the cavity vessels, and the static losses on the 5-K and 80-K circuits have been derived from the temperature (i.e., enthalpy) rises of the average shield temperatures after stopping the coolant flow. A dozen of temperature sensors were installed on each thermal shield of the module in order to perform these measurements. Temperature sensors were also placed at thermal sinks in order to analyze the heat load contributions of individual conduction paths.

The good agreement between estimations and measurements in the S1-Global experiment, which has been made possible to the large amount of diagnostics planned and handled during the test cool-downs by the KEK team, is another confirmation that the module design is well understood in terms of its thermal behavior and design options of subcomponents can be explored by means of suitably detailed FEM models in order to derive their thermal performances with a reasonable error margin. Other studies have been performed in the past also to benchmark transient behavior during cooldown, with similar agreement [12].

Table 3.1 is also a useful example to illustrate the opportunity of value engineering and overall optimization for a complex system as the ILC cryomodule. For example, Module-A was equipped with better-grade RF cables for the HOM and Wire Position Monitors (WPM) sensors, resulting in an increased heat leak to the 2-K environment. The use of external motor drives for the tuner action to allow replacement without dismounting the module (as a measure to reduce maintanance times) introduces additional heat loads to the cavity environment. The different coupler designs also have different thermal performances due to different design choices (e.g. the STF-2 coupler design, contrary to the TTF-III, has no bellows between the 5-K and 70-K intercepts to simplify clean roam assembly) , and this fact should be factored when considering mechanically "plug-compatible" component design.

A third important activity carried by the S1-Global collaboration has been the

Table 3.1: Comparison of static S1-Global module heat load estimations with measurements.

Temperature	Component	Module-A [W]	Module-C [W]
2-K	Thermal radiation	≈0.0	≈ 0.0
	Input couplers (4×)	0.29	0.08
	HOM RF, Piezo cables	2.1	0.71
	Tuner driving shafts (4×)	0.48	NA
	Temperature sensor wires	0.18	
	WPM, pin diodes wires	1.72	0.82
	WPM connection pipe	0.17	≈0.0
	Support posts (2×)	0.25	
	Beam Pipe	0.02	<0.01
Total Estimated 2-K load at module		5.2	2.1
Total Estimated 2-K load (both modules)		7.3 (6.8 without support posts)	
Total Measured 2-K load (both modules)		7.2	
5-K	Thermal radiation	0.66	0.68
	Input couplers (4×)	4.00	0.92
	Support posts (2×)	1.54	
	Sensor wires	0.9	
	Beam Pipe	0.1	0.05
Total Estimated 5-K load at module		7.2	4.1
Total Measured 5-K load at module		7.3	5.3
80-K	Thermal radiation	16.6	15.9
	Input couplers (4×)	9.60	7.28
	Support posts (2×)	10.78	
	RF cables	6.88	1.30
	Sensor wires	0.08	
	Beam Pipe	0.37	0.10
Total Estimated 80-K load at module		44.4	35.3
Total Measured 80-K load at module		48.7	34.4

assessment of the cavity and coupler dynamic loads during module testing. This has been achieved by a sequence of four measurements of static and dynamic loads of each cavity on resonance and in detuning conditions, evaluated from the flow rate of evaporated LHe. All cavities were driven to high field values (25-38 MV/m) with a Q_0 estimated from this analysis in the range $\approx 4 - 9 \times 10^9$. These measurements were then repeated by driving simultaneously all four cavities in each of the modules, leading to the heat load values reported in Table 3.2. The extensive temperature diagnostics implemented in the modules showed that the different behavior in the coupler dynamic loads in the two modules was associated to a substantial temperature increase at the interconnection flange between the STF-2 couplers and the cavity port. The temperature rise is originated at the Cu layer of 3 µm thickness on the inner surface of the outer conductor. The measurement taken at S1-Global were instrumental for a redesign of the Quantum Beam cryomodule couplers at KEK with a different coating procedure and more performant thermal anchoring to reduce the static and dynamic heat losses.

Table 3.2: S1-Global RF dynamic heat load measurements.

	Module C 4 cavities		Module A 4 cavities	
	resonant	detuned	resonant	detuned
Gradient MV/m	20	32	26.9	32
Total RF load, W	2.7	NA	6.9	NA
Coupler dynamic load, W	0.2	0.5	2.5	4.6
Cavity RF load, W	2.5	NA	4.4	NA

3.1.2 Measurements of the thermal performances of the XFEL prototype modules

(**Author:** *this section should be reviewed by B.Petersen once completed)*

The European XFEL has started the procurement of the 100 cryomodules for its accelerator. All modules will be thoroughly tested for their RF and cryogenic performances at the Accelerator Module Test Facility (AMTF) in DESY before tunnel installation, and will yield a copious amount of data with a statistical significance for the ILC.

An update of all static heat load evaluations for the XFEL module design, integrating the minor changes introduced with respect to the Type-III TTF modules, has been performed at DESY [13] and compared to the thermal performances of the XFEL prototype modules, assessed experimentally at the DESY CryoModule Test Facility (CMTB).

Thermal loads have been assessed and measured several times, under different operating conditions, as a function of the outer shield temperature (which varies along the cryostring). The heat loads in the 2-K region are evaluated from the mass flow rate of the evaporated helium during the tests, while the loads on the 5-K and 80-K circuits are evaluated from the helium coolant flow conditions and cross-checked with the enthalpy response of the cold mass. A separate test with a dummy module was performed to separate the heat loads of the end/feed caps of the CMTB from that of the module.

Table 3.3 lists the updated heat transfer evaluations (for current leads, power couplers, support posts, thermal radiation, . . .) and the comparison with the measured values of the three protytpes, which are also shown in Fig. 3.1, along with the budget values foreseen by the refrigerator.

Table 3.3: XFEL updated static heat load evaluation.

Temperature level	Static heat load, W,	
	Evaluated	Measured
2-K	2.1	3.5-6
5-8 K	6-12	6-11
40/80 K	100-120	100-120

Generally speaking, measured values agree with calculated values for the 5/8 K and 40/80 K circuits. The increase in heat loads in the outer shields during the PXFEL3 (A) test has been traced to an improper tuner assembly operation, which caused a thermal contact. The lower 40/80 K heat loads shown by the the PXFEL2_1 measurements seems to suggest a better performances of the new MLI blankets that have been used for this test.

The measured values for the 2-K environment deviate from the evaluations due to an underestimation of the cabling heat loads and, furthermore, vary strongly mainly due to the installation skill of the quadrupole current leads. The high static loads of PXFEL1 have been traced to an incorrect layout of a prototype current lead.

As for the S1-Global measurements, the XFEL experience shows that it is possible to predict thermal performances of cryomodules with reasonable error margins, but great attention need to be paid in the details of the models, which need to include all heat transfer mechanism. Furthermore, care needs to be placed in the assembly procedures, in order to avoid spurious heat load increases resulting from incorrect operations. Figure 3.1 clearly show also a “training” effect for the most sensitive 2-K environment, showing a decrease in time of measured heat loads. One of the crucial outcomes of the European XFEL AMTF test towards the ILC consolidation would be the confirmation of this trend for the testing of the series modules.

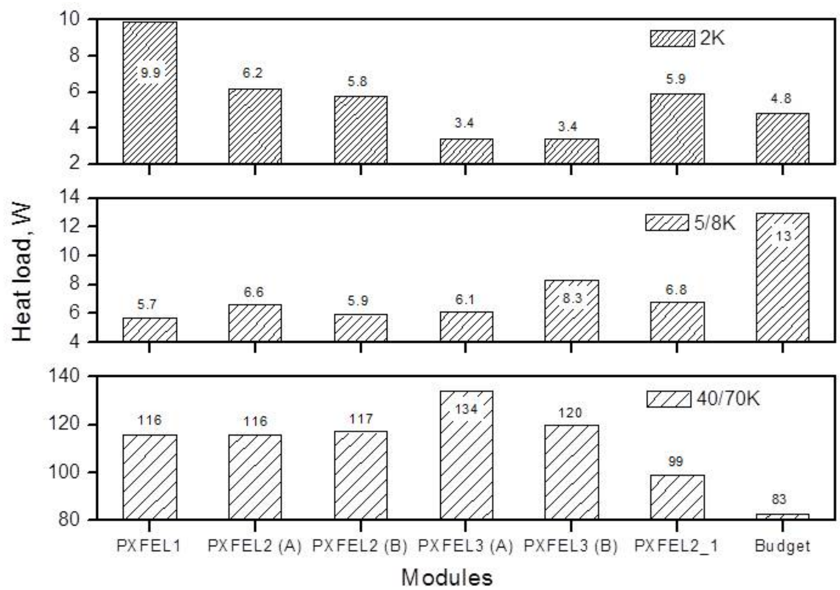

Figure 3.1: XFEL Prototype heat load measurements at CMTB, compared to the budget values (from [13]).

3.1.3 Measurements of the thermal performances of the NML CM1 (1-2 pg)

(**Author:** *We discussed it by phone. Thermal measurements were performed also at FNAL, we can have a small subsection from FNAL. TP? 1 to 2 pages?)*

3.1.4 Cryogenic thermal balance and Baseline TDR cryomodule

The design and experimental activities described in this section, and in particular those achieved with the S1-Global module characterization and with the testing of European XFEL pre-series modules, show that the ILC module concept is well understood and proven, leaving further possible refinements to be introduced at the conclusive engineering stage of the project, where the combined cryomodule/cryosystem layout will be finely tuned for overall efficiency and cost reduction for the large production. The activity in the Technical Design Phase has confirmed that the thermal behavior of the module and its subcomponents can be reliably estimated with numerical models to explore design variants and simplifications, in order to draw a deal between design complexity and thermal performance, or to account for possible reliability-driven requirements (as, for example, the possibility, if needed, to simplify the access to the cold mass for subcomponent replacement without the complete module removal, at the cost of increased heat losses). The European XFEL will also provide a substantial amount of expertise from the AMTF operation with the series module testing in the coming years.

The baseline ILC TDR cryomodule is therefore almost unchanged from the description provided in the RDR, with a unique slot length of 12.652 m for the two main variants (nine cavity module and eight cavity plus quadrupole module) . The present baseline relies also on the use of a conduction-cooled split quadrupole, as discussed in the following paragraph.

3.1.5 R&D on the split quadrupole

Superconducting linear accelerators have a number of cryomodules with superconducting quadrupole magnets for beam focusing and steering. Various superconducting magnet designs have been investigated for superconducting linacs. Nearly all existing magnet designs are bath cooled by LHe and they need to be assembled with the string of superconducting RF (SCRF) cavities inside a clean room, leading to the risk of particle contamination of the cavity surfaces and to increased chances of cavity performance deterioration. Akira Yamamoto, as the ILC Project Manager, proposed to investigate for the ILC cryomodule design a conduction-cooled splittable quadrupole. The splittable magnet can then be assembled around the beam pipe after all SCRF cavities are installed and sealed inside the clean room. In this case the magnet will never enter the clean room and its installation will not lead to the risk of contaminating the SCRF cavity inner surfaces. The splittable quadrupole was designed and built at Fermilab, and tested in a 4.4 K helium bath at the FNAL Magnet Test Facility (MTF).

The main issue for the ILC quadrupole is to provide magnetic axis stability of a few (5) µm during a -20% focusing field change. This requirement arises from the Beam Based Alignment (BBA) technique, a procedure to determine the electron beam position relative to quadrupole magnetic center and adjust dipole correctors to move the beam on center. The magnetic and mechanical effects which correlate with the magnetic axis stability must be eliminated.

Table 3.4 shows the specification and design parameters for the splittable quadrupole shown in Fig. 3.2. The quadrupole has a vertical split plane and is assembled from two half cores having racetrack superconducting coils on magnet poles. The magnet halves are tightened to each other by stainless steel bandage rings. This assembly is surrounded by Al thermal leads which have a good thermal contact with the cryomodule LHe supply line. The LHe line provides the cooling by conduction to this cryogen free magnet [14].

Table 3.4: Splittable quadrupole magnet specifications and parameters.

Parameter	Value	Unit
Peak gradient	54	T/m
Integrated gradient	36	T
Peak operating quadrupole current	100	A
Magnet total length	680	mm
SC wire diameter	0.5	mm
NbTi filament size (vendor value)	3.7	µm
Cu:SC volume ratio	1.5	
Superconductor Critical current (5 T and 4.2 K)	200	A
Coil maximum field at 100 A current	3.3	T
Magnetic field stored energy	40	kJ
Quadrupole inductance	3.9	H
Quadrupole coil number of turns/pole	900	
Yoke outer diameter	280	mm

The fabrication and test of a splittable quadrupole confirmed the design concept. Figure 3.3 shows the quadrupole on the vertical test insert ready for measurement in pool bath mode at FNAL. After training up to 110 A, the magnet reached 20% current margin, as shown in Fig. 3.4, and the specified peak gradient of 54 T/m was reached at 90 A. The quadrupole center position shift over a 20% gradient change is shown in Fig. 3.5 as a function of the nominal operating current,and only exceeds slightly the specifications of 5 µm on the horizontal plane at currents in the 30–70 A range. More careful control of the yoke gap size and uniformity may improve this. Future plans are to improve the magnet split plane flatness to eliminate small gaps, and test again in a conduction-cooling mode. (**Author:** *The magnet is now at KEK for the conduction cooled tests. Is there something new on this?)*

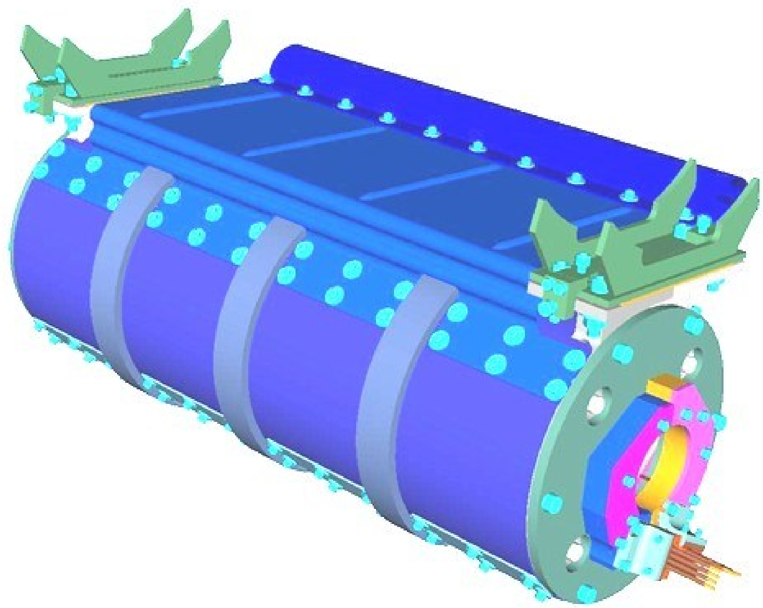

Figure 3.2: The split quadrupole final assembly.

Figure 3.3: The split quadrupole mounted on the insert of the cryostat.

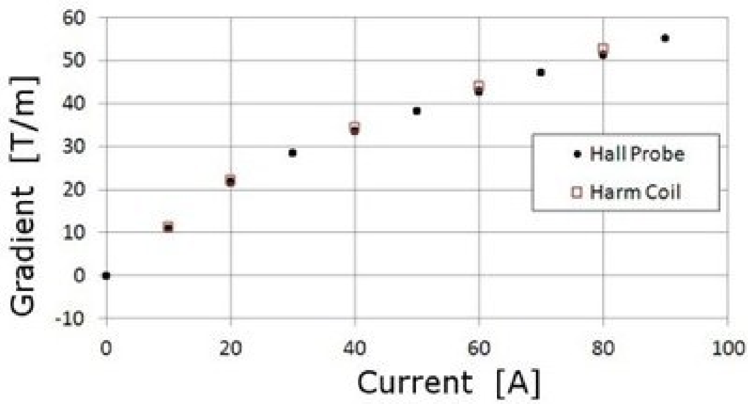

Figure 3.4: The quadrupole gradient as a function of current.

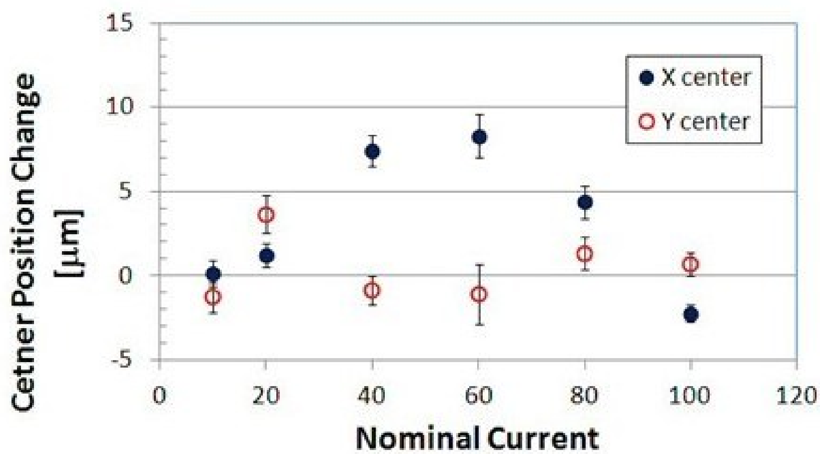

Figure 3.5: The magnetic center shift as a function of current.

Bibliography

[1] "TESLA Technical Design Report, March 2001. TESLA Report 2001-23" `http://flash.desy.de/tesla/tesla_documentation/#e1509`

[2] C. Pagani, J. G. Weisend II, R. Bandelmann, D. Barni, A. Bosotti, G. Grygiel, H. Kaiser, U. Knopf, F. Loeffler, P. Pierini, O. Peters, B. Petersen, D. Sellmann, S. Wolff, "Construction, Commissioning and Cryogenic Performances of the First TESLA Test Facility (TTF) Cryomodule," Advances in Cryogenic Engineering, Vol. 43 (1998).

[3] D. Barni, C. Pagani, P. Pierini, "Towards the Third Generation of TTF Cryomodule," TESLA 1998-16, `http://flash.desy.de/reports_publications/tesla_reports/tesla_reports_1998/`

[4] N. Phinney, N. Toge and N. Walker (*Eds.*) "International Linear Collider Reference Design Report Volume 3: Accelerator," arxiv:0712.2361 [physics.acc-ph]. ILC-REPORT-2007-001

[5] E. Elsen, M. Harrison, L. Hesla, M. Ross, P. Royole-Degieux, R. Takahashi, N. Walker, B. Warmbein, A. Yamamoto, K. Yokoya, M. Zhang (*Eds.*), "The International Linear Collider: A Technical Progress Report," ILC-REPORT-2011-030

[6] N. Ohuchi *et al.*, "Plan of the S1-Global Cryomodules for ILC," PAC-2009-we6rfp005 (2009), *Presented at the 23rd Particle Accelerator Conference (PAC 2009), Vancouver, Canada, 4-8 May 2008, p. 2790*, JACoW: `PAC2009/papers/we6rfp005.PDF`

[7] N. Ohuchi *et al.*, "S1-Global Collaborative Efforts - 8-Cavity-Cryomodule: 2 FNAL, 2 DESY and 4 KEK," LINAC-2010-mo302 (2010), *Presented at the Linear Accelerator Conference (LINAC 2010), Tsukuba, Japan, 12-17 September 2010, p. 31*, JACoW: `LINAC10/PAPERS/mo302.PDF`

[8] N. Ohuchi *et al.*, "Construction of the S1-Global Cryomodules for ILC," IPAC-2010-wepe008 (2010), *Presented at the First International Particle Accelerator Conference (IPAC 2010), Kyoto, Japan, 23-28 May 2010, p. 3356*, JACoW: `IPAC10/mo302.PDF`

[9] D. Kostin *et al.*, "S1-Global Module Tests at STF/KEK," IPAC-2011-mooda02 (2011), *Presented at the Second International Particle Accelerator Conference (IPAC 2011), San Sebastian, Spain, 4-9 September 2011, p. 38*, JACoW: `IPAC11/papers/mooda02.PDF`

[10] N. Ohuchi *et al.*, "Thermal Performance of the S1-Global Cryomodule for ILC," IPAC-2011-wepo035 (2011), *Presented at the Second International Particle Accelerator Conference (IPAC 2011), San Sebastian, Spain, 4-9 September 2011, p. 2472*, JACoW: `IPAC11/papers/wepo035.PDF`

[11] N. Ohuchi *et al.*, "The First Cool-Down Test of the 6 meter-long Cryomodules for Superconducting RF Test Facility (STF) at KEK," EPAC-2008-mopp144, *Presented at the Eleventh European Particle Accelerator Conference (EPAC2008), Genova, Italy, 23-27 June, 2008, p. 892,* JACoW: `e08/papers/mopp144.pdf`

[12] S. Barbanotti, P. Pierini, K. Jensch, R. Lange, W. Maschmann, "Thermal and Structural Modeling of the TTF Cryomodule Cooldown and Comparison with Experimental Data," EPAC-2008-wepd038, *Presented at the Eleventh European Particle Accelerator Conference (EPAC2008), Genova, Italy, 23-27 June, 2008, p. 2494,* JACoW: `e08/papers/wepd038.pdf`

[13] X.L. Wang, W: Maschmann, J. Eschke, O. Sawlanski, R. Klos, K. Jensch, B. Petersen, "Thermal Performance Analysis and Measurements for the Accelerator Prototype Modules of European XFEL," *Presented at the TESLA Technology Collaboration Meeting, IHEP, Bejing, China, 5-8 December, 2011*

[14] V.S. Kashikhin, N. Andreev, J. Kerby, Y. Orlov, N. Solyak, M. Tartaglia, G. Velev, "Superconducting Splittable Quadrupole Magnet for Linear Accelerators", *Presented at the 22nd International Conference on Magnet Technology (MT22), Marseille, France, 12-16 September 2011*

List of Figures

List of Tables